瘻孔の閉鎖には基本的に骨片と筋膜を用い、フィブリン糊で接着した。瘻孔に対しては真珠腫のない部位から剥離を始め、慎重に瘻孔上の母膜を剥離した。骨迷路のみ破壊されている場合はまず骨片を置き、その上を筋肉片や筋膜で被覆した。膜迷路に病変が及んでいる場合は半規管内を筋肉片や筋膜弁で充填し、その上を骨片で被覆する方法をとった。

結　　果

1．初診時主訴と自覚症状

初診時主訴はめまいが8例と最も多く、42%を占めていた。難聴および耳閉が6例、耳漏が4例であった（表1）。症状別の割合では、難聴は全例にあり、耳漏は15例(79%)、めまいは12例(63%)にあった。顔面神経麻痺は1例であった。瘻孔症状があったのは7例（37%）であった（図1）。

2．真珠腫の存在部位

真珠腫の存在部位は日本耳科学会により提案された進展範囲に基づいて分類した[6]。上鼓室・乳突洞が11耳、上鼓室・鼓室・乳突洞が1耳、上鼓室・前鼓室・乳突洞が5耳、上鼓室・前鼓室・鼓室・乳突洞すべてにあったものが2耳であった。

3．瘻孔の存在部位と大きさ

瘻孔の存在部位は後半規管瘻孔の1例を除き、すべて外側半規管であった。大瘻孔が12耳(63%)、小瘻孔は7耳（37%）であった。顔面神経管の露出は14耳（74%）に認められた。

4．聴力、めまいと瘻孔の大きさとの関係

術前の気導聴力は11例（58%）が高度難聴であった。平均気導聴力は75.6 dB、骨導聴力は39.7dBであった。骨導聴力が正常な症例は6例(32%）であった（図2）。聴力と瘻孔の大きさの関係では、大瘻孔の平均聴力は64.4 dB、小瘻孔は94.6 dBで、瘻孔の大きさと聴力は関連せず、小瘻孔に聴力低下例が多い印象であった（図3）。

めまい症状は大瘻孔で7例（58%）、小瘻孔で5例（71%）にみられ、瘻孔の大きさに関係なく比較的高頻度であった（図4）。瘻孔症状は大瘻孔で6例（50%）、小瘻孔で1例（14%）にみられた(図3)。瘻孔症状が不明であるのは緊急手術や大量の耳漏などで検査が十分に行えなかった例である。

5．術式

術式は外耳道後壁削除鼓室形成術が16耳、うちIII型5耳、IV型6耳、wo型5耳であった。またすべての症例で外耳道後壁の再建を行った。外耳道後壁保存鼓室形成術は1耳でwo型であった。一期的に手術を行えたものは14耳で、二期的に行ったのは3耳であった。また2耳で中耳根本術を行った。

6．聴力改善成績

日本耳科学会の聴力改善の成績判定案[7]に基づき、気導聴力の成績判定を行った。聴力評価が可能であったのは16耳であった。聴力改善を意図して手術した8耳の再建方法はIII型変法が3耳、IV型変法が5耳で、5耳（63%）が成功耳となった（表2）。骨導平均聴力を比較すると10 dB以上改善したのは3耳あり、うち1耳は15 dB以上の改善であった。15 dB以上悪化したものはなかった。

7．前庭症状

めまい症状は12例にあったが、術後経過とともに全例消失した。また耳漏も全例停止した。

考　　察

半規管瘻孔は真珠腫性中耳炎の合併症の一つであり、手術症例の約10%に認められる[1),2)]。内耳の開放は骨導聴力を悪化させると考えられていたが、病変の郭清によって改善したという報告もある[3)]。真珠腫の手術において半規管瘻孔をいかに取り扱うかは、真珠腫の完全摘出、聴力保存、めまいのコントロールなど異なった要素を考慮しなければならないだけに重要である。

今回検討した症例の年齢は11歳から80歳に及んだ。50－60歳代が最も多かったが、11歳例も1例あった。この症例は、多発性の側頭骨骨欠損が自然閉鎖した症例として以前報告した[8)]。小児

表1　初診時主訴

症状	症例数
めまい	8例
難聴	5例
耳漏	4例
耳閉感	1例
頭痛	1例

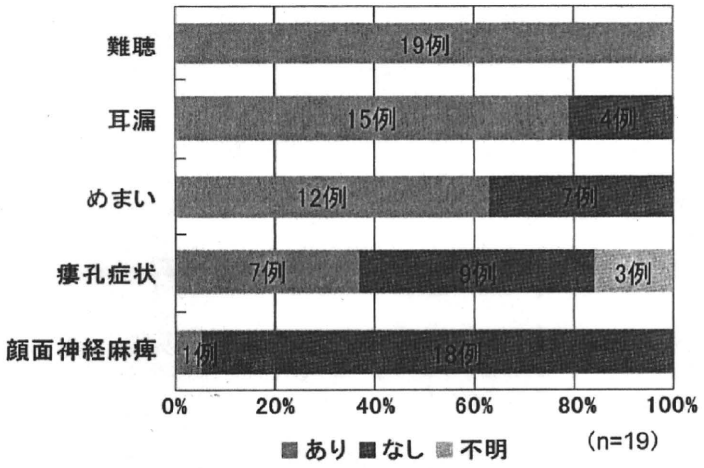

図1　自覚症状

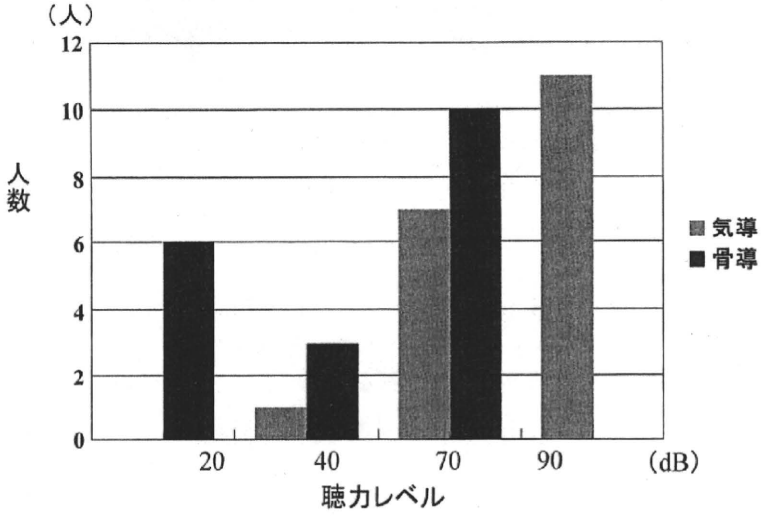

図2　術前聴力

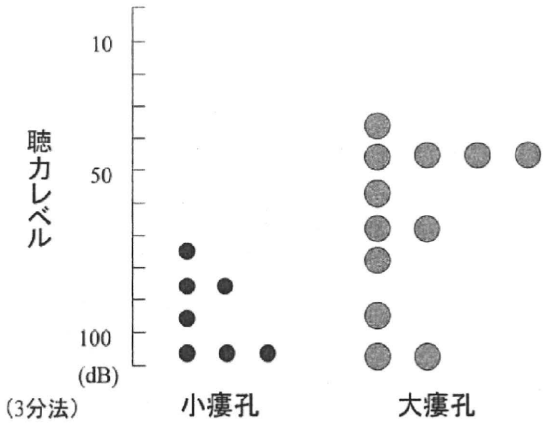

図3　瘻孔の大きさと聴力

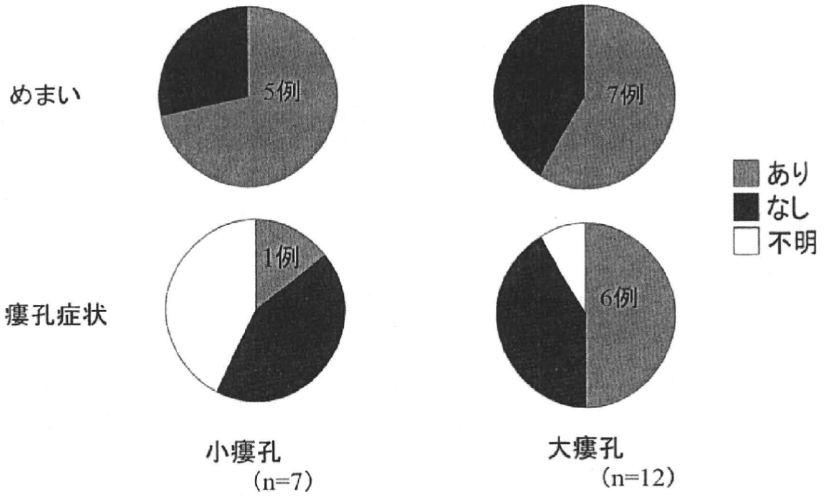

図4　めまいと瘻孔症状

表2　気導聴力評価

	全症例	伝音再建あり
改善	5耳	5耳
不変	8耳	3耳
悪化	3耳	0耳
	16耳	8耳

例では骨が柔らかく、真珠腫で骨欠損がある場合は瘻孔が存在する可能性を念頭におく必要がある。

主訴としてはめまいが最多であったが、瘻孔症状は37%と予想より少なかった。瘻孔部が厚い組織で覆われていたり、瘻孔周囲に固い瘢痕組織などが存在したりする場合は瘻孔症状が現れ難いものと想像された。また、外側半規管機能が著明に低下した場合も瘻孔症状が出ない可能性がある。症状全体でみると、めまいは63%にあり、瘻孔以外にも内耳炎が比較的高率に存在することがうかがわれた。耳漏も79%と多く、感染を伴う真珠腫が瘻孔を来しやすいことが考えられた。乾燥耳よりも湿潤耳で真珠腫増大の速度が早いことが報告されており[9),10)]、特に耳漏のある例では瘻孔を含む骨欠損の進展度に注意を払うべきである。

術前の気導聴力は半数以上が高度難聴であった。しかしながら、骨導聴力が正常範囲の例も32%あり、一方でめまい症状は比較的多いことから蝸牛系と前庭系とで内耳炎の波及程度に差があることが考えられた。

真珠腫の存在部位は、予想どおり上鼓室中心であった。今回は、真珠腫が広範囲の症例が多かったこともあり、弛緩部型と緊張部型に分けた検討は行っていないが、上鼓室・前鼓室・鼓室・乳突洞すべてに存在した症例などは少なくとも緊張部型真珠腫が進展した例であったと思われる。

瘻孔のサイズについての報告は多い[4),5),11),12)]。われわれの症例では、大瘻孔の頻度が高かった。しかしながら、結果で述べたように瘻孔のサイズと術前聴力に関連はなく、むしろ小瘻孔に聴力低下例が多かった。聴力に影響するのは内耳炎の病態や程度であることを考えると、瘻孔のサイズよりもその深さなどほかの要素が聴力を左右するものと思われる。めまい症状も聴力と同様、小瘻孔に高頻度にみられた。瘻孔症状の頻度は大瘻孔で約半数と高く、これは単純に瘻孔が大きくなるほど外耳道圧が半規管に伝わりやすいためと考えられた。なお、今回は、緊急手術、多量の耳漏などの理由で温度刺激検査が施行されていない症例が多く、温度眼振については解析しなかったが、少なくとも瘻孔症状のある症例では温度眼振反応はある程度保たれていたものと推測される。

聴力改善を意図した症例での聴力改善率は63%でおおむね満足できる結果であった。ただし、術前気導聴力が悪い症例が多いことを考えると、聴力改善結果と患者本人の満足度とは必ずしも一致するものでないことは容易に想像される。今後は、患者自身の満足度を加味した聴力評価法も必要となろう。術後の骨導聴力の改善についてはこれまで報告されており[3),12),13)]、主として内耳炎のコントロールによるものとされている。今回の検討では骨導聴力は3耳で改善しており、そのうち1耳は15 dB以上の改善であった。骨導聴力悪化予防の意味でも早期の瘻孔閉鎖が望ましいと考える。なお、めまいは術後全例で消失した。高齢者の場合、内耳性めまいが転倒の一つの原因になり得る。転倒予防の意味からも積極的に瘻孔を処置しておくことが望ましいと考える。

瘻孔の処置法については以前から議論されている[3),14),15)]。注意深く母膜を除去し、速やかに瘻孔を閉鎖するのが基本的な手技と思われる。内骨膜が残っている場合や外リンパが漏出する程度の状態であれば、そのまま瘻孔を閉鎖することでまず聴力に影響はないと考えられる。瘻孔閉鎖材料には骨片、筋膜などが使われている。われわれは、原則として薄い骨片でまず閉鎖し、その上を筋膜で覆う方法をとっている。多くの骨欠損は自然閉鎖する傾向があることから、軟組織の被覆で十分とする報告もある[2)]。われわれも巨大な骨欠損が自然閉鎖した小児真珠腫例を経験し、報告した[6)]。しかしながら、骨欠損部が自然閉鎖するにしてもそれが完了するにはある程度の期間を要すること、軟組織で被覆した後も瘻孔症状を数カ月間訴えていた症例を以前経験したこと、材料の種類で閉鎖手技自体に影響はないことなどから、われわれは原則としてまず骨片を使用することにしてい

る。

瘻孔閉鎖手技自体は聴力へ悪影響を及ぼさないことは知られている。BPPVに行う半規管遮断術の後も聴力低下はまれであることを考えると[16]、たとえ瘻孔部に筋膜などの組織を充填しても、感染がなく、ごく局所的な充填であれば聴力に問題はないと思われる。今回聴力改善を目的としなかった症例の中には、瘻孔部に深く肉芽が入り込んでおり、それを除去した後、筋膜片を半規管内に挿入したケースがあった。これは、Dornhoffer分類のIIIに相当する膜迷路障害例と思われる[17]。このような場合は肉芽をある程度引きずり出すような手技をとらざるを得ず、膜迷路障害や聴力低下の可能性が高くなる。大瘻孔や経過の長い瘻孔であるほどその可能性が増すので、予測される場合は術前に十分説明を行っておくことが望まれる。特に良聴耳の際は細心の手術手技と十分な術前説明が必要で、場合によっては母膜を意図的に瘻孔部に残し、2次的に処理する方法[3),14)]や、小川[2)]が述べるように外来で定期的な真珠腫debris除去を続け、真珠腫の進展予防を図る方法も考慮する必要がある。

なお、本論文の要旨は第19回日本耳科学会総会学術講演会で発表した。

文　献

1) Quaranta N et al：Surgical treatment of labyrinthine fistula in cholesteatoma surgery. Otolaryngol Head Neck Surg **140**：406-411, 2009.
2) 小川　郁：側頭骨外科：どこまで危険部位に迫れるか. 内耳瘻孔の取り扱い. 頭頸部外科 **18**：103-108, 2008.
3) 小林俊光他：術後に骨導聴力の著明な改善をみた真珠腫による迷路瘻孔－2症例の報告－. 耳喉 **57**：379-384, 1985.
4) Gacek R R et al：The surgical management of labyrinthine fistulae in chronic otitis media with cholesteatoma. Ann Otol Rhinol Laryngol **83**：1-19, 1974.
5) 斎藤春雄他：迷路瘻孔と術後聴力. 耳鼻臨床 **72**：3-7, 1979.
6) 日本耳科学会用語委員会：中耳真珠腫の進展度分類について（2008）. Otol Jpn **18**：611-615, 2008.
7) 日本耳科学会用語委員会：聴力改善の成績判定について（2000）. Otol Jpn **11**：62-63, 2001.
8) 長谷川達哉他：頭蓋底骨欠損が自然閉鎖した中耳真珠腫症例. Otol Jpn **18**：52-58, 2008.
9) 鈴木　衛他：真珠腫遺残性再発例の検討. 耳鼻 **40**：937-940, 1994.
10) Ruedi L：Acquired cholesteatoma. Arch Otorhinolaryngol **78**：252-261, 1963.
11) 片平　文他：慢性中耳炎による迷路瘻孔と内耳機能. 耳喉 **55**：617-621, 1983.
12) 前田　学他：慢性中耳炎手術症例における迷路瘻孔の検討. 耳鼻臨床 **89**：1065-1070, 1996.
13) 奥野秀次他：真珠腫性中耳炎における術前・術後の骨導閾値の変化について. 耳鼻 **38**：225-229, 1992.
14) 飯野ゆき子他：真珠腫による内耳瘻孔症例の術後聴力. 耳鼻臨床 **88**：31-36, 1995.
15) 森　京子他：中耳真珠腫における半規管瘻孔－瘻孔部位と術後聴力－. Otol Jpn **19**：173-178, 2009.
16) Suzuki M et al：Clinical effect of canal plugging on paroxysmal positional vertigo with lateral canal lesion. J Laryngol Otol **114**：959-962, 2000.
17) Dornhoffer JL and Milewski C：Management of the open labyrinth. Otolaryngol Head Neck Surg **112**：410-414, 1995.

（受付　2009年10月22日急載）

Clinical observation of a semicircular canal fistula associated with cholesteatoma

Eriko SHINADA, Mamoru SUZUKI, Sachie KAWAGUCHI, Nobuhiro NISHIYAMA, Akira HAGIWARA, Yasuo OGAWA and Atsushi KAWANO

Department of Otorhinolaryngology, Tokyo Medical University, Tokyo 160-0023, Japan

Nineteen cases of labyrinthine fistulae associated with cholesteatoma were analyzed. Either vertigo or dizziness was the most frequent symptom, followed by hearing loss and ear fullness. Fistula symptoms were present in 37% of the cases. Fistulae measuring greater than 2 mm in size were found in 12 cases (63 %). All fistulae, except for one posterior semicircular canal fistula, were found in the lateral semicircular canal. The average air and bone conduction levels prior to surgery were 72.5 dB and 37.4 dB, respectively. The preoperative hearing level was not related to the size of the fistulae. The bone conduction improved in 3 cases after surgery. No case showed any hearing deterioration after surgery. Our main surgical procedure includes a careful dissection of the matrix over the fistula followed by sealing with a piece of bone and fascia. The symptoms of either vertigo or dizziness disappeared in all cases. To improve hearing and the control vertigo, the early treatment of labyrinthine fistulae is therefore recommended.

ELSEVIER

Auris Nasus Larynx 37 (2010) 742–746

AURIS NASUS LARYNX
INTERNATIONAL JOURNAL OF ORL & HNS

www.elsevier.com/locate/anl

A case of apogeotropic nystagmus with brainstem lesion: An implication for mechanism of central apogeotropic nystagmus

Takao Imai [a,*], Arata Horii [b], Noriaki Takeda [c], Tadashi kitahara [a], Kayoko Higashi-Shingai [d], Hidenori Inohara [a]

[a] *Department of Otorhinolaryngology - Head and Neck Surgery, Osaka University Graduate School of Medicine, 2-2 Yamadaoka, Suita-shi, Osaka 565-0871, Japan*
[b] *Department of Otolaryngology, Suita Municipal Hospital, Osaka, Japan*
[c] *Department of Otolaryngology, University of Tokushima, School of Medicine, Tokushima, Japan*
[d] *Department of Otolaryngology, Osaka Seamen's Insurance Hospital, Osaka, Japan*

Received 15 November 2009; accepted 9 April 2010
Available online 26 June 2010

Abstract

We report a case showing apogeotropic nystagmus with the lesion of the brain stem, and discuss a possible mechanism of central apogeotropic nystagmus. The case was a 73-year-old male. We analyzed his nystagmus three-dimensionally. He showed apogeotropic nystagmus. Axis angles of slow phase eye velocity of his apogeotropic nystagmus were not in line with the axes perpendicular to the plane of horizontal semicircular canals, but with the patient's vertical axis. We then found that his nystagmus including the apogeotropic nystagmus was positioning, but not positional and that the direction of his positioning nystagmus was the same direction of postrotatory nystagmus after his head movement. His MRI scans showed an infarction around the prepositus hypoglossi nucleus of the brain. His apogeotropic nystagmus seemed to consist of a combination of prolonged postrotatory nystagmus after his head rotation to the left and right lateral position because the axis of postrotatory nystamus was in line with the axis of the head rotation. Therefore, it is suggested that a possible mechanism of central apogeotropic nystagmus is a prolonged postrotatory nystagmus after his head movement in the supine position due to the brain lesion involving the velocity storage mechanisms.

Keywords: Cupulolithiasis; Rotation vector; Infrared CCD camera; Velocity storage; Positioning nystagmus

1. Introduction

Nystagmus beating to the right at the left lateral position and beating to the left at right lateral position in the supine position is an apogeotropic positional nystagmus, which was traditionally thought to be caused by central vestibular lesions such as cerebellar infarction [1–3]. Recently, it has been demonstrated that most apogeotropic positional nystagmus was of benign peripheral origin, namely a subtype of benign paroxysmal positional vertigo (BPPV), and that the cupulolithiasis of the horizontal semicircular canal (HSCC) is the cause of this nystagmus [4,5].

We encountered a case of intractable positional nystagmus which was very similar to the HSCC type of BPPV (H-BPPV), an apogeotropic nystagmus, with a small lesion in the central vestibular system. We report a patient and discuss a possible mechanism of central apogeotropic nystagmus.

2. Patients and methods

The patient was a 73-year-old male, who experienced brief episodes of positional and positioning vertigo and showed horizontal apogeotropic nystagmus triggered by head rotation to both then left and right in the supine position. His positional and positioning nystagmus was

* Corresponding author. Tel.: +81 6 6879 3951; fax: +81 6 6879 3959.
E-mail address: imaitakao@hotmail.com (T. Imai).

0385-8146/$ – see front matter
doi:10.1016/j.anl.2010.04.004

analyzed three-dimensionally. He had no other evidence of neurologic diseases, but MRI scans showed an old infarction of the brain stem around the prepositus hypoglossi nucleus (PPHN). His apogeotropic nystagmus continued for more than 1600 days.

To compare central apogeotropic nystagmus with peripheral apogeotropic nystagmus, we also analyzed positional nystagmus three-dimensionally in another case of a 70-year-old male with H-BPPV. His apogeotropic nystagmus disappeared within 29 days and MRI scans of his brain showed no lesions.

Positional and positioning nystagmus of the left eye was recorded on videotape with an infrared CCD camera (*RealEyes*, Micromedical Technologies). The videotape images were converted into digital images (720 dot × 480 dot) (*PCV-R63K*, SONY) and the space coordinates of the center of the pupil and an iris freckle were reconstructed in three dimensions. The analysis method of the eye rotation vector and its accuracy has already been described elsewhere [6,7]. For the space coordinates, the *X*-axis was parallel to the naso-occipital axis (positive forward), the *Y*-axis was parallel to the inter-aural axis (positive left), and the *Z*-axis was normal to the *X*–*Y* plane (positive upwards). *X*, *Y*, and *Z* components mainly reflect roll, pitch, and yaw components, respectively. We used the unit of degree that is given as $2 \times \tan^{-1}$(magnitude of rotation vector) to represent the eye position as axis-angle representations [8]. Using $\mathbf{r}$ as the rotation vector of eye position and the following formula: $\omega = 2 \times (d\mathbf{r}/dt + \mathbf{r} \times d\mathbf{r}/dt)/(1 + \mathbf{r}^2)$, we calculated the eye velocity ω [9]. We then extracted the slow phase eye velocity (SPEV) of the nystagmus by the method based on a fuzzy set approach [10,11]. Using the least squares method, SPEV against time was approximated exponentially. Finally, the time constant was calculated as the reciprocal of the coefficient of time.

3. Results

MRI scans of the patient's brain demonstrated a small infarction from the basal pons to the upper medulla, containing PPHN (arrow head in Fig. 1A).

The patient showed apogeotropic nystagmus when the head was turned to left (left column in Fig. 1B) or right (right column in Fig. 1B) in the supine position. The time constant of SPEV in Z component was 59.5 and 81.7 s when his head was rotated from head centered supine position to left and right lateral head position, respectively (Fig. 1B).

We found that his nystagmus was not positional, but positioning. Firstly, when he moved from sitting to the head centered supine position, the nystagmus mainly existed in the *Y* component (vertical component), of which the direction was downward (Fig. 2A). The time constant of SPEV in Y component was 20.3 s (inserted graph in Fig. 2A). Secondly, when he turned from the left lateral position to the head centered supine position, the nystagmus

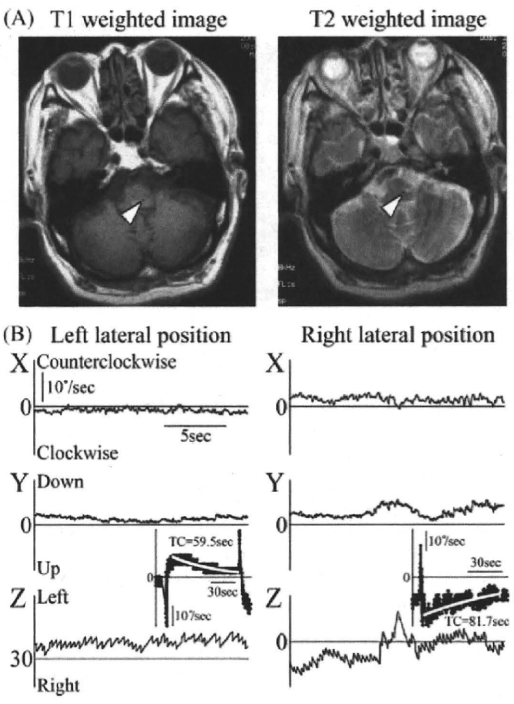

Fig. 1. (A) Images of MRI scans. Open triangle: an infarction around PPHN. (B) Apogeotropic nystagmus. Rightward nystagmus on left lateral head position and leftward nystagmus on right lateral head position in the supine position. Inserted graph shows the axis angles of SPEV in Z component. The time constant (TC) was 59.5 and 81.7 s when his head was rotated from head centered supine position to left and right lateral head position, respectively.

mainly existed in the *Z* component (horizontal component), of which the direction was leftward (Fig. 2B). Thirdly, when he turned from the right lateral position to the head centered supine position, the nystagmus mainly existed in the *Z* component, of which the direction was rightward (Fig. 2C). Finally, when he moved from the head centered supine position to sitting, the transient nystagmus mainly existed in the *Y* component, of which the direction was upward (open triangle in Fig. 2D). The time constant of SPEV in *Y* component was 1.0 s (inserted graph in Fig. 2D). But, when he moved very slowly from sitting to the head centered supine position again, no nystagmus was induced (data not shown). These findings demonstrated that the direction of his positioning nystagmus in the head centered supine position was dependent on the path of his head movement and was the same direction of postrotatory nystagmus after his head movement.

Axis angles of SPEV of his apogeotropic nystagmus were plotted in *XY*, *XZ*, and *YZ* planes (Fig. 3A). The averaged lines of the axis angles were calculated and shown as dotted lines. The dotted lines in *XZ* and *YZ* planes were not in line with the axes perpendicular to the plane of right (Rh) and left HSCCs (Lh) [12], but with the vertical axis.

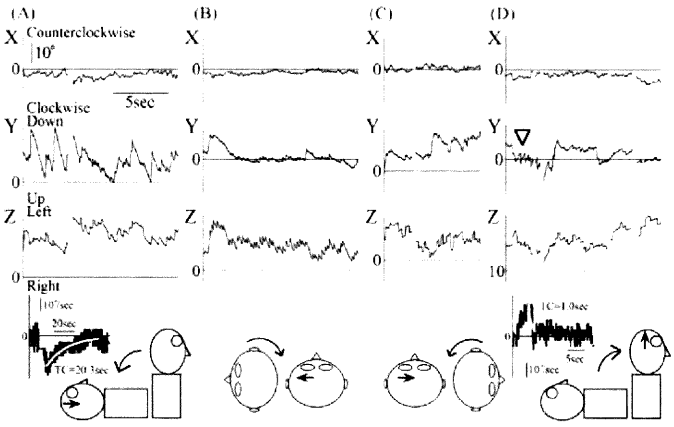

Fig. 2. Positioning nystagmus. (A) When he moved from sitting to the head centered supine position, the nystagmus mainly existed in the *Y* component, of which the direction was downward. (B) When he turned from the left lateral position to the head centered supine position, the nystagmus mainly existed in the *Z* component, of which the direction was leftward. (C) When he turned from right lateral position to the head centered supine position, the nystagmus existed in the *Z* component, of which the direction was rightward. (D) When he moved from the head centered supine position to sitting, the transient nystagmus existed in the *Y* component, of which the direction was upward (open triangle). Inserted graph shows the axis angles of SPEV in *Y* component. The time constant (TC) was 20.3 s when he moved from sitting to the head centered supine position and 1.0 s when he moved from the head centered supine position to sitting.

Axis angles of SPEV of his positioning nystagmus when the patient moved from sitting to the head centered supine position and from the head centered supine position to sitting were plotted in *XY*, *XZ*, and *YZ* planes (Fig. 3B). The averaged lines shown by dotted lines in *XY* and *YZ* planes were in line with the horizontal axis.

To compare central apogeotropic nystagmus with peripheral apogeotropic nystagmus, we then analyzed positional nystagmus three-dimensionally in another patient with H-BPPV. The patient showed apogeotropic positional nystagmus when the head was turned to the left or right in the supine position (Fig. 4A). When his head was in the head centered

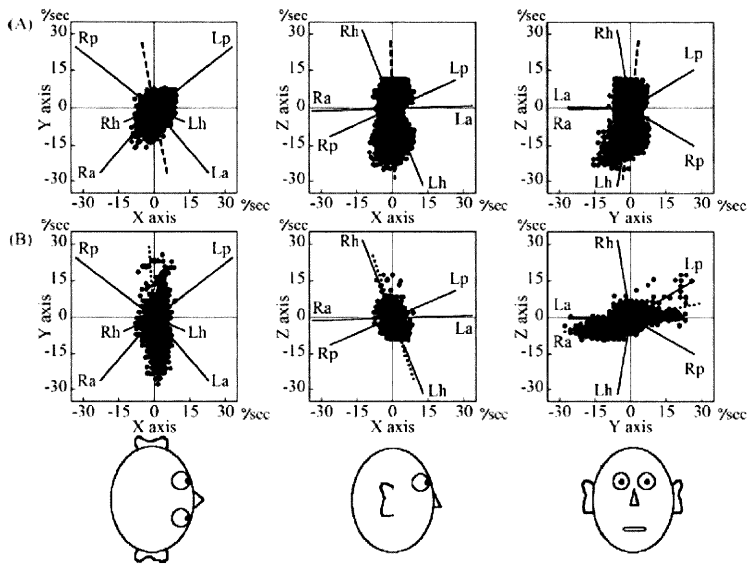

Fig. 3. Axis angles of SPEV in *XY*, *XZ*, and *YZ* planes. (A) Axis angles of SPEV of apogeotropic nystagmus. The axis angles of SPEV were plotted around the vertical axis. The dotted line means the average line calculated from the axis angles. Ra, axis of right anterior semicircular canal; Rh, axis of right HSCC; Rp, axis of right posterior semicircular canal; La, axis of left anterior semicircular canal; Lh, axis of left HSCC; Lp, axis of left posterior semicircular canal [12]. (B) Axis angles of SPEV of positioning nystagmus. When he moved from sitting to the head centered supine position and from the head centered position to sitting. The axis angles of SPEV were plotted around the horizontal axis.

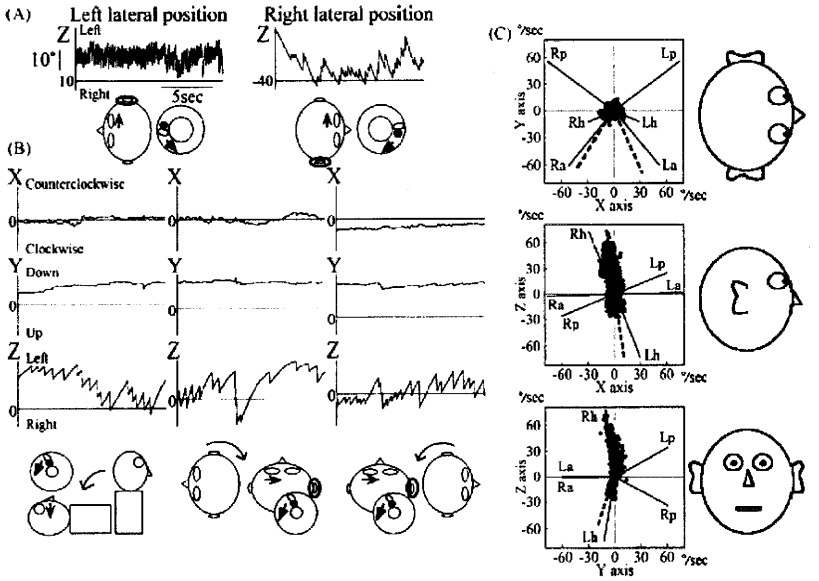

Fig. 4. (A) Apogeotropic nystagmus in the patient with H-BPPV (B) Positional nystagmus in the patient with H-BPPV. First column: when he moved from sitting to the head centered supine position, the nystagmus was rightward. Second column: when he turned from left lateral position to the head centered supine position, his nystagmus was rightward. Third column: when he turned from right lateral position to the head centered supine position, his nystagmus was rightward. Inserted figures in (A) and (B) show head position and right HSCC. The filled circle in the HSCC shows cupulolithiasis. The direction of the arrow around the eye in the figure shows the direction of fast phase of positional nystagmus. The direction of the arrow in the HSCC shows the direction of deflection of cupula. (C) Axis angles of SPEV of positional nystagmus including apogeotropic nystagmus in *XY*, *XZ*, and *YZ* planes in the patient with H-BPPV. The abbreviations are the same in Fig. 2B. The axis angles of SPEV were plotted around Rh and Lh. The dotted line means the average line calculated from the axis angles of SPEV.

supine position, regardless of the path of change of his head, he showed rightward positional nystagmus, not positioning nystagmus (Fig. 4B). Axis angles of SPEV of his apogeotropic nystagmus and his nystagmus when his head was moved to the head centered supine position were plotted in *XY*, *XZ*, and *YZ* planes (Fig. 4C). The averages shown by dotted lines in the *XZ* and *YZ* planes were in line with Rh and Lh.

4. Discussion

In the present study, we report a patient showing central apogeotropic nystagmus with a lesion in the brainstem. The case showed apogeotropic positional nystagmus (Fig. 1B). We then found that his nystagmus was not positional, but positioning, and that the direction of his nystagmus in the head centered supine position was dependent on the path of his head movement (Fig. 2). Since the direction of his positioning nystagmus was opposite to the direction of the nystagmus induced by vestibulo-ocular reflex (VOR) during his head movement to the head centered supine position and the same direction of postrotatory nystagmus after his head movement, these findings lead to the possibility that his apogeotropic nystagmus is postrotatory nystagmus, occurring after his head rotation.

To prove the possibility, we analyzed his apogeotropic nystagmus three-dimensionally. When his head was rotated from head centered supine position to left or right lateral position, and from left or right lateral position to head centered supine position, the axis angles of SPEV of his apogeotropic nystagmus was plotted around the vertical axis, which is consistent with the axis of the head rotation (Fig. 3A). When his head was moved from sitting to the head centered supine position, and from the head centered supine position to sitting, the axis angles of SPEV of his positioning nystagmus were plotted around the horizontal axis, which is in line with the axis of the head movement (Fig. 3B). These findings suggest that the positioning nystagmus including apogeotropic nystagmus is prolonged postrotatory nystagmus. In other words, his apogeotropic nystagmus seemed to consist of a combination of prolonged rightward postrotatory nystagmus after his head rotation to the left lateral position and prolonged leftward postrotatory nystagmus after his head rotation to the right lateral position in the supine position.

In this case, MRI scans demonstrated a brainstem lesion, which was involved in PPHN. It was reported that PPHN was included in the neural network of the velocity storage mechanism that was associated with preservation of vestibular inputs and prolongation of vestibular outputs [13,14]. The velocity storage mechanism could explain that postrotatory

nystagmus declines exponentially with a longer time constant than that of the cupula [15]. In this case, inhibitory pathways from the cerebellum to PPHN may be disturbed by the brainstem lesion and then the velocity storage mechanisms may be enhanced, resulting in prolonged postrotatory nystagmus of the central apogeotropic nystagmus.

Finally, we compared the central apogeotropic nystagmus with peripheral apogeotropic nystagmus in another patient with H-BPPV. The patient showed apogeotropic nystagmus (Fig. 4A). His nystagmus was positional, but not positioning and his apogeotropic nystagmus was explained by cupulolithiasis in the right HSCC (Fig. 4B). At the head centered supine position, regardless of the path of his head movement, positional nystagmus beating to the right was induced by the cupulolithiasis of the right HSCC as shown by inserted figures in Fig. 4B. The axis angles of SPEV of his positional nystagmus, including apogeotropic nystagmus, was plotted around the lines perpendicular to the plane of left or right HSCC (Fig. 4C).

In conclusion, we proposed a possible mechanism of central apogeotropic nystagmus that consists of a combination of prolonged postrotatory nystagmus after head rotation in the supine position. The prolonged time constant of postrotatory nystagmus may be caused by dysfunction of the velocity storage mechanisms due to brainstem lesion.

Acknowledgment

We thank Dr. Kazuhiro Teramoto for his helpful advice.

References

[1] Fernandez C, Fredrickson JM. Experimental cerebellar lesions and their effect on vestibular function. Acta Otolaryngol Suppl 1964;192:53–62.

[2] Sakata E, Uchida Y, Nakano Y, Takahashi K. Pathophysiology of positional vertigo of the malignant paroxysmal type. Auris Nasus Larynx 1984;11:79–90.

[3] Brandt T. Central positional vertigo. In: Brandt T, editor. Vertigo. Its multisensory syndromes. 1st ed., London: Springer-Verlag; 1991. p. 165–70.

[4] Casani A, Giovanni V, Bruno F, Luigi GP. Positional vertigo and ageotropic bi-directional nystagmus. Laryngoscope 1997;107:807–13.

[5] Imai T, Takeda N, Sato G, Sekine K, Ito M, Nakamae K, et al. Changes in slow phase eye velocity and time constant of positional nystagmus at transform from cupulolithiasis to canalolithiasis. Acta Otolaryngol (Stockh) 2008;128:22–8.

[6] Imai T, Takeda N, Morita M, Koizuka I, Kubo T, Miura K, et al. Rotation vector analysis of eye movement in three dimensions with an infrared CCD camera. Acta Otolaryngol (Stockh) 1999;119:24–8.

[7] Imai T, Sekine K, Hattori K, Takeda N, Koizuka I, Nakamae K, et al. Comparing the accuracy of video-oculography and the scleral search coil system in human eye movement analysis. Auris Nasus Larynx 2005;32:3–9.

[8] Raphan T. Modeling control of eye orientation in three dimensions. I. Role of muscle pulleys in determining saccadic trajectory. J Neurophysiol 1998;79:2653–67.

[9] Haslwanter T. Mathematics of three-dimensional eye rotations. Vision Res 1995;35:1727–39.

[10] Arzi M, Mignin M. A fuzzy set theoretical approach to automatic analysis of nystagmic eye movements. IEEE Trans Biomed Eng 1989;36:954–63.

[11] Naoi K, Nakamae K, Fujioka H, Imai T, Sekine K, Takeda N, et al. Three-dimensional eye movement simulator extracting instantaneous eye movement rotation axes, the plane formed by rotation axes, and innervations for eye muscles. IEICE Trans Inf Syst 2003;11:2452–62.

[12] Blanks RHI, Curthoys IS, Markham CH. Planar relationships of the semicircular canals in man. Acta Otolaryngol (Stockh) 1975;80:185–96.

[13] Raphan T, Matsuo V, Cohen B. Velocity storage in the vestibulo-ocular reflex arc (VOR). Exp Brain Res 1979;35:229–48.

[14] Yokota J, Reisine H, Cohen B. Nystagmus induced by electrical stimulation of the vestibular and prepositus hypoglossi nuclei in the monkey: evidence for site of induction of velocity storage. Exp Brain Res 1992;92:123–38.

[15] Leigh RJ, Zee DS. In: Leigh RJ, Zee DS, editors. The vestibular-optokinetic system. The neurology of eye movements. 3rd ed., New York: Oxford University Press; 1999. p. 19–89.

Acta Oto-Laryngologica, 2010; 130: 1135–1140

informa
healthcare

ORIGINAL ARTICLE

Clinical characteristics of delayed endolymphatic hydrops in Japan: A nationwide survey by the Peripheral Vestibular Disorder Research Committee of Japan

HIDEO SHOJAKU[1], YUKIO WATANABE[1], NORIAKI TAKEDA[2], TETSUO IKEZONO[3], MASAHIRO TAKAHASHI[4], AKINOBU KAKIGI[5], JUICHI ITO[6], KATSUMI DOI[7], MAMORU SUZUKI[8], MASAYA TAKUMIDA[9], KATSUMASA TAKAHASHI[10], HIROSHI YAMASHITA[11], IZUMI KOIZUKA[12], SHINICHI USAMI[13], MITSUHIRO AOKI[14] & HIDEAKI NAGANUMA[15]

[1]*Departments of Otolaryngology, University of Toyama,* [2]*University of Tokushima,* [3]*Nihon Medical University,* [4]*Yokohama Central Clinic,* [5]*University of Kochi,* [6]*University of Kyoto,* [7]*University of Osaka,* [8]*Tokyo Medical University,* [9]*University of Hiroshima,* [10]*University of Gunma,* [11]*University of Yamaguchi,* [12]*St Marianna Medical University,* [13]*University of Sinsyu,* [14]*University of Gifu and* [15]*Kitasato University, Japan*

Abstract

Conclusion: Similarly to almost all delayed endolymphatic hydrops (DEH) cases with both precedent sudden deafness and mumps deafness, two-thirds of DEH cases with precedent deafness of unknown cause with onset in early childhood developed DEH symptoms within 40 years after the precedent deafness. In spite of the diagnosis of precedent deafness, viral labyrinthitis may build up the late endolymphatic hydrops in most DEH cases up to four decades. *Objective:* To clarify the characteristics of DEH in Japan. *Methods:* Clinical information on 198 DEH cases was collected by nationwide, multicenter surveys conducted by the Peripheral Vestibular Disorders Research Committee of Japan. *Results:* The incidence of the ipsilateral type of DEH was 47.5%, which was almost equal to that of the contralateral type. In both types of DEH, the most common diagnosis of precedent deafness was deafness of unknown cause with onset in early childhood: 43.9% in both types of DEH. Sudden deafness and mumps deafness were the subsequent diagnoses of precedent deafness. The distribution of time delay of the onset between precedent deafness of unknown cause with onset in early childhood and DEH was different from that between precedent sudden and mumps deafness and DEH.

Keywords: *Ipsilateral, contralateral, cause of profound hearing loss, onset age, Time delay of onset between precedent deafness and DEH*

Introduction

Clinical characteristics of delayed endolymphatic hydrops (DEH) have been reported from around the world [1–16]. Most such reports are derived from clinical records at a single facility, and do not employ statistical analysis because DEH is relatively rare compared with Meniere's disease. The Meniere's Disease Research Committee of Japan was organized by the Ministry of Health and Welfare of Japan in 1974 and continued after reorganization in 1980 as the Peripheral Vestibular Disorders Research Committee. To investigate the epidemiologic and clinical characteristics of DEH, the committee conducted nationwide, multicenter surveys of patients admitted to the hospitals where members of the committee were affiliated five times in 1998, 2001, and 2006–2008.

Correspondence: Hideo Shojaku, Department of Otolaryngology, University of Toyama, 2630 Sugitani, Toyama 930-0194, Japan. Tel: +81 764 34 7368. Fax: +81 764 34 5038. E-mail: hshojaku@med.u-toyama.ac.jp

(Received 28 December 2009; accepted 22 February 2010)

ISSN 0001-6489 print/ISSN 1651-2251 online
DOI: 10.3109/00016481003745513

DEH is classified into ipsilateral and contralateral types. The diagnostic criteria for DEH in Japan were proposed by the committee of the Japan Society for Equilibrium Research in 1987 [17]. The criteria used for the diagnosis of the ipsilateral type of DEH are as follows: (1) a precedent event characterized by profound sensorineural hearing loss in one ear (precedent deafness); (2) delayed development of episodic attacks of vertigo without fluctuating hearing loss in the opposite ear; and (3) exclusion of central nervous system lesions, eighth nerve tumors, and other cochleovestibular diseases such as syphilitic labyrinthitis. The criteria used for the diagnosis of the contralateral form of DEH are as follows: (1) precedent deafness in one ear; (2) delayed development of fluctuating hearing loss in the opposite ear that is sometimes associated with episodic attacks of vertigo; and (3) exclusion of central nervous system lesions, eighth nerve tumors, and other cochleovestibular diseases like syphilitic labyrinthitis. Profound hearing loss was defined as a pure tone average of greater than 90 dB over the 500, 1000, and 2000 Hz frequencies.

In 5 nationwide, multicenter surveys, the same diagnostic criteria have been used consistently and data for 198 patients with DEH were collected. In the present study, the rate of ipsilateral versus contralateral type of DEH, the sex ratio, diagnosis of precedent deafness, age at the onset of precedent deafness, age at the onset of DEH, and time delay of the onset between precedent deafness and DEH were analyzed.

Material and methods

The first nationwide survey was conducted from June to November 1998 by seven committee members at seven university hospitals in Japan. Data were collected from 60 patients with DEH. The second nationwide survey was conducted from January to December 2001 by 11 committee members in 11 university hospitals. The third to the fifth surveys were conducted annually from January 2006 to December 2008 by 18 committee members at 1 private and 13 university hospitals. From the 5 nationwide, multicenter surveys, data from a total of 198 patients with DEH were assembled.

Survey data were stored and analyzed by database software at the Department of Otolaryngology at the University of Toyama. Data from the five surveys on the age and sex distribution of DEH, the rate of ipsilateral versus contralateral type of DEH, the diagnosis of the precedent deafness, age at onset of precedent deafness, age at onset of DEH, the time delay of onset between preceding deafness and onset of DEH were analyzed. For statistical analysis, Student's *t* tests and chi-square tests were performed with StatView for Windows (version 4.5, Abacus Concepts, Berkeley, CA, USA).

Results

According to the criteria proposed by the committee of the Japan Society for Equilibrium Research, 198 patients with DEH were diagnosed as 94 cases (47.5%) of the ipsilateral type of DEH, and as 104 cases (52.5%) of the contralateral type of DEH. The number of patients with each type of DEH was almost equal (Table I). Among the patients with the contralateral type of DEH, 18 (17.3%) complained of fluctuating hearing loss in the opposite ear to the precedent deafness without vertigo, while 86 cases (82.7%) complained of fluctuating hearing loss in the opposite ear to the precedent deafness with vertigo.

A slight female predominance was observed in both types of DEH (Table I). For the ipsilateral type of DEH, there were 43 males (45.7%) and 51 females (54.3%) and for the contralateral type of DEH there were 39 males (37.5%) and 64 females (61.5%).

Among the 94 patients with the ipsilateral type of DEH, the diagnosis of precedent deafness was deafness of unknown cause in 57 cases (60.6%), sudden deafness in 15 cases (16.0%), and mumps in 9 cases (9.6%) (Table II). Deafness of unknown cause was found early in childhood (i.e. deafness of unknown cause with onset in early childhood) in 41 cases (43.6%). Among the 104 patients with the contralateral type of DEH, the diagnosis of precedent deafness

Table I. Sex ratio and symptoms of delayed endolymphatic hydrops (DEH).

Parameter	Ipsilateral type	Contralateral type	Total
Total no. of patients	94	104	198
Males	43 (45.7%)	39 (37.5%)	82 (41.4%)
Females	51 (54.3%)	64 (61.5%)	115 (58.1%)
Unknown		1 (1.0%)	1 (0.5%)
Fluctuating hearing loss with vertigo	-	86 (82.7%)	-
Fluctuating hearing loss without vertigo	-	18 (17.3%)	

Table II. Diagnosis of precedent deafness in DEH.

Parameter	Ipsilateral type	Contralateral type	Total
Cause unknown	57 (60.6%)	65 (62.5%)	122 (61.6%)
Onset in early childhood	41 (43.6%)	46 (44.2%)	87 (43.9%)
Onset age ≥ 5 years	10 (10.6%)	15 (14.4%)	25 (12.6%)
Onset unknown	6 (6.4%)	4 (3.9%)	10 (5.1%)
Sudden deafness	15 (16.0%)	10 (9.6%)	25 (12.6%)
Mumps deafness	9 (9.6%)	15 (14.4%)	24 (12.5%)
Otitis media and mastoiditis	8 (8.5%)	8 (7.7%)	16 (8.1%)
Streptomycin injection	1 (1.1%)	1 (1.0%)	2 (1.0%)
Meningitis	1 (1.1%)	1 (1.0%)	2 (1.0%)
Surgery	0	2 (1.9%)	2 (1.0%)
Measles	1 (1.1%)	0	1 (0.5%)
High fever	1 (1.1%)	0	1 (0.5%)
Head trauma	1 (1.1%)	0	1 (0.5%)
Inner ear abnormality	0	1 (1.0%)	1 (0.5%)
Meniere's disease	0	1 (1.0%)	1 (0.5%)
Total no. of patients	94	104	198

was deafness of unknown cause in 65 cases (62.6%), sudden deafness in 10 cases (9.6%), and mumps deafness in 15 cases (14.4%) (Table II). Deafness of unknown cause with onset in early childhood was found in 46 cases (44.2%). In both types of DEH, the three main diagnoses of the precedent deafness were deafness of unknown cause, sudden deafness, and mumps deafness. For deafness of unknown cause, deafness of unknown cause with onset in early childhood was the most common diagnosis.

In the ipsilateral type of DEH, the mean age at the onset of precedent deafness was 1.8 years in cases with deafness of unknown cause with onset in early childhood, 44.9 years in cases with sudden deafness, and 4.0 years in cases with mumps deafness (Table III). In the contralateral type of DEH, the mean age at the onset of precedent deafness was 2.3 years in cases with deafness of unknown cause with onset in early childhood, 31.6 years in cases with sudden deafness, and 5.5 years in cases with mumps deafness (Table IV). In both types of DEH, age at the onset of precedent deafness in cases with sudden deafness was significantly older than that with deafness of unknown cause with onset in early childhood and mumps deafness.

In the ipsilateral type of DEH, the mean age at the development of DEH was 28.1 years in cases with precedent deafness of unknown cause with onset in early childhood, 57.6 years in cases with precedent sudden deafness, and 24.1 years in cases with precedent mumps deafness (Table III). In the contralateral

Table III. Time delay of onset between precedent deafness and DEH in patients with the ipsilateral type of DEH among the three main diagnoses of precedent deafness.

Parameter	No. of patients	Age at onset of precedent deafness (years)	Age at onset of DEH (years)	Time delay of onset between precedent deafness and DEH (years)
Total no. of patients	94	14.5 (19.9)	38.9 (19.8)	23.9 (15.2)
Cause unknown with onset in early childhood	41	1.8 (1.5)*+	28.1 (14.8)*+	26.4 (14.8)*+
Sudden deafness	15	44.9 (16.5)*+	57.6 (15.0)*+	13.7 (10.8)*+
Mumps deafness	9	4.0 (2.6)+	24.1 (9.9)+	19.9 (8.8)

Results are shown as mean (SD).
*+$p < 0.01$.

Table IV. Time delay of onset between precedent deafness and DEH in patients with the contralateral type of DEH among the three main diagnoses of precedent deafness.

Parameter	No. of patients	Age at onset of precedent deafness (years)	Age at onset of DEH (years)	Time delay of onset between precedent deafness and DEH (years)
Total no. of patients	104	11.1 (15.9)	39.2 (17.8)	26.7 (16.9)
Cause unknown with onset in early childhood	46	2.3 (1.3)	31.9 (16.3)†	29.7 (16.3)*
Sudden deafness	10	31.6 (16.9)*	48.8 (10.2)*†	16.8 (11.1)*†
Mumps deafness	15	5.5 (4.4)*	22.7 (9.2)*	17.2 (10.2)

Results are shown as mean (SD).
*$p < 0.01$.
†$p < 0.05$.

type of DEH, the mean age at the development of DEH was 31.9 years in cases with precedent deafness of unknown cause with onset in early childhood, 48.8 years in cases with precedent sudden deafness, and 22.7 years in cases with precedent mumps deafness (Table IV). In both types of DEH, age at the development of DEH in cases with precedent sudden deafness was significantly older than that with precedent deafness of unknown cause with onset in early childhood and mumps deafness.

In the ipsilateral type of DEH, the mean time delay of the onset between precedent deafness and DEH was 26.4 years in cases with deafness of unknown cause with onset in early childhood, 13.7 years in cases with sudden deafness, and 19.9 years in cases with mumps deafness (Table III). In the contralateral type of DEH, the mean time delay of the onset between precedent deafness and DEH was 29.7 years in cases with deafness of unknown cause with onset in early childhood, 16.8 years in cases with sudden deafness, and 17.2 years in cases with mumps deafness (Table IV). In both types of DEH, the time delay of the onset between precedent deafness and DEH in cases with deafness of unknown cause with onset in childhood was significantly longer than that with precedent sudden deafness.

The distribution of the time delay of the onset between precedent deafness and DEH in cases with deafness of unknown cause with onset in early childhood, sudden, and mumps deafness is shown in Table V. A chi-square test showed that the distribution of the time delay of the onset between precedent deafness and DEH in cases with unknown cause with onset in early childhood was different from that with sudden and mumps deafness (vs sudden deafness $p < 0.01$; vs mumps deafness $p < 0.05$). However, in 58 of 87 (72.8%) cases with precedent deafness of unknown cause with onset in early childhood, in 24 (96%) of 25 cases with precedent sudden deafness, and in 24 cases (100%) with precedent mumps deafness, DEH symptoms developed up to 40 years. Thus, two-thirds of DEH cases with precedent deafness of unknown cause with onset in early childhood developed DEH symptoms up to 40 years after precedent deafness, like almost all DEH cases with both precedent sudden and mumps deafness.

Table V. Distribution of time delay of onset between precedent deafness and DEH among the three main diagnoses of precedent deafness.

Time delay (years)	Cause unknown with onset in early childhood	Sudden deafness	Mumps deafness
0.9	3 (2.4%)	8 (32%)	4 (16.7%)
10–19	24 (27.6%)	9 (36.0%)	9 (37.5%)
20–29	16 (18.4%)	5 (20.0%)	8 (33.3%)
30–39	15 (17.2%)	2 (8.0%)	3 (12.5%)
40–49	5 (5.7%)	1 (4.0%)	0
50–59	17 (19.5%)	0	0
≥60	7 (8.0%)	0	0
Total	87	25	24

Chi-square test showed the difference of the distribution of time delay of onset between unknown cause with onset in early childhood and sudden deafness ($p < 0.01$) or mumps deafness ($p < 0.05$).

Discussion

A total of 549 cases with unilateral DEH were previously reported [1–16]. Before the first publication of the criteria for the contralateral type of DEH by Schuknecht [4], 116 cases with the ipsilataral type of DEH had been reported. After Schuknecht's study, a total of 439 cases with DEH were documented, including 293 cases with the ipsilateral type of DEH and 140 cases with the contralateral type of DEH. The morbidity that causes vertigo is the same in both types of DEH. The discrepancy in the proportion of the contralateral type of DEH among the previous studies was likely caused by differences in the diagnostic criteria for the contralateral type of DEH used in each study, rather than by regional differences. In the contralateral type of DEH, the hearing level of the opposite better-hearing ear fluctuates for a long time after the onset of precedent profound deafness [4]. Some patients with the contralateral type of DEH suffered from fluctuating hearing loss with vertigo, others did not experience the symptom. In previous studies including patients both with and without vertigo [6,7,9,10,13,14], the mean rate of the contralateral type of DEH was 40.5%. However, in previous studies that included only patients with vertigo [5,8,11,12,15,16], the mean rate of the contralateral type of DEH was 25.2%. In the present study, because the contralateral type of DEH was diagnosed in patients with and without vertigo according to the criteria proposed by the Committee of the Japan Society for Equilibrium Research, the rate of the contralateral type of DEH was increased to 52.3%. Among them, 82.7% of patients were with vertigo and 17.3% of patients were without vertigo.

In the previous studies [1–16], the diagnoses of precedent deafness in a total of 549 cases with DHE were as follows: in the ipsilateral type of DEH, the diagnosis of precedent deafness was deafness of unknown cause with onset in early childhood in 198 cases (32.3%), sudden deafness in 58 cases (14.2%), and mumps in 63 cases (13.4%). In the contralateral type of DEH, the diagnosis of precedent deafness was deafness of unknown cause with onset in early childhood in 63 cases (45.0%), sudden deafness in 14 cases (10%), and mumps in 7 cases (5.0%). In the present study, the diagnosis of the precedent deafness of the ipsilateral type of DEH was deafness of unknown cause with onset in early childhood in 41 cases (43.6%), sudden deafness in 15 cases (16.0%), and mumps deafness in 9 cases (9.6%). The diagnosis of the precedent deafness of the contralateral type of DEH was deafness of unknown cause with onset in early childhood in 46 cases (44.2%), sudden deafness in 10 cases (9.6%), and mumps deafness in 15 cases (14.4%). The present findings demonstrated that in both types of DEH, the most common diagnosis of the precedent deafness was deafness of unknown cause with onset in early childhood, and that sudden and mumps deafness are the two main subsequent diagnoses of precedent deafness, which was consistent with the previous reports.

In both types of DEH, the mean age at the onset of precedent deafness in cases with sudden deafness was significantly older than that in cases with both deafness of unknown cause with onset in early childhood and mumps deafness (Tables III and IV). Therefore, the mean age at the development of DEH in cases with precedent sudden deafness was significantly older than in cases with precedent deafness of unknown cause with onset in early childhood and mumps deafness (Tables III and IV).

In the present study, in both types of DEH, the mean time delay of the onset between precedent sudden deafness and DEH did not differ from that between precedent mumps deafness and DEH (Tables III and IV). In contrast, the mean time delay of the onset between precedent deafness of unknown cause with onset in early childhood and DEH was significantly longer than that between precedent sudden deafness and DEH. These findings suggest that the mechanism of the development of DEH after deafness of unknown cause with onset in early childhood is different from that after sudden and mumps deafness. In 1985, Schuknecht [18] proposed a mechanism for the development of DEH: viral labyrinthitis damages the endolymph resorptive system during precedent deafness, resulting in endolymphatic hydrops long after the onset of precedent deafness. Since viral labyrinthitis has been supposed as an etiology of sudden deafness [19], in cases with precedent sudden and mumps deafness, DEH may develop under the mechanism proposed by Schuknecht. In fact all DEH cases, with the exception of one case with precedent sudden and mumps deafness, developed DEH symptoms within 40 years after the precedent deafness (Table V).

Distribution of time delay of the onset between precedent deafness of unknown cause with onset in early childhood and DEH was significantly different from that between precedent sudden and mumps deafness and DEH. However, like almost all DEH cases with both precedent sudden and mumps deafness, two-thirds of DEH cases with precedent deafness of unknown cause with onset in early childhood developed DEH symptoms within 40 years of the precedent deafness (Table V). Since viral labyrinthitis has been supposed as an etiology of deafness of unknown cause with onset in early childhood [1,10], the present findings suggest that, in spite of

the diagnosis of precedent deafness, the viral labyrinthitis may build up the late endolymphatic hydrops in most DEH cases up to four decades.

The pathogenesis of Meniere's disease is idiopathic endolymphatic hydrops. Based on the nationwide surveys from 2001 to 2006 conducted by the Peripheral Vestibular Disorders Research Committee in Japan [20], age at onset of Meniere's disease peaked in the fifth decade in males and the sixth decade in females. In the present study, the remaining one-third of DEH cases with precedent deafness of unknown cause with onset in early childhood developed DEH symptoms over 40 years after the precedent deafness. The development of DEH symptoms in such cases at more than 40 years old may be associated with the occasional Meniere's disease.

DEH is one of the secondary endolymphatic hydrops. Several etiologic factors other than viral infection have been reported in the generation of the endolymphatic hydrops [21–23]. Suzuki et al. [23] reported that 5 (28%) of 18 cases with deafness of unknown cause with onset in early childhood, 1 (100%) case with ipsilateral type of DEH, and 6 (75%) of 8 cases with the contralateral type of DEH showed the presence of autoantibody against inner ear protein. The wider distribution of the time delay of the onset between precedent deafness of unknown cause with onset in early childhood and DEH than that between precedent sudden and mumps deafness and DEH might be related to another etiologic factor, such as the autoimmune response.

Acknowledgments

This work was supported by a grant from the Ministry of Health, Labor and Welfare of Japan. We express our sincere appreciation to all members of the Department of Otolaryngology, University of Toyama, for their assistance and cooperation.

Declaration of interest: The authors report no conflicts of interest. The authors alone are responsible for the content and writing of the paper.

References

[1] Kamei T, Noro H, Yabe T, Makino S. Statistical observation of unilateral total deafness and characteristic unilateral total deafness among young children with tendency towards occurrence of dizziness. Jibiinkoka 1971;43:349–58.

[2] Nadol JB, Weiss AD, Parker SW. Vertigo of delayed onset after sudden deafness. Ann Otol Rhinol Laryngol 1975;84:841–6.

[3] Wolfson RJ, Liebermann A. Unilateral deafness with subsequent vertigo. Laryngoscope 1975;85:1762–6.

[4] Schuknecht HF. Delayed endolymphatic hydrops. Ann Otol 1978;87:743–8.

[5] LeLiever WC, Barber HO. Delayed endolymphatic hydrops. J Otolaryngol 1980;9:375–80.

[6] Kudo Y, Senba T, Futaki T. Delayed endolymphatic hydrops. Diagnosis and treatment. Pract Otol (Kyoto) 1986;(Suppl 8):208–16.

[7] Hicks GW, Wright JW. Delayed endolymphatic hydrops: a review of 15 cases. Laryngoscope 1988;98:840–5.

[8] Inokari I, Takahashi M, Ito M. Delayed endolymphatic hydrops. Case report and statistical observation. Otolaryngol Head Neck Surg (Tokyo) 1988;60:369–75.

[9] Watanabe Y, Aso S, Mizukoshi K. Clinical findings of delayed endolymphatic hydrops. Characteristics of contralateral cases. Equilibrium Res (Kyoto) 1989;(Suppl 5):152–7.

[10] Schuknecht HF, Suzuka Y, Zimmermann C. Delayed endolymphatic hydrops and its relationship to Meniere's disease. Ann Otol Rhinol Laryngol 1990;99:843–53.

[11] Yoshida T, Kitsuda C, Kimura Y, Harada K, Yamamoto M, Oda M. Statistical analysis of delayed hydrops. Equilibrium Res (Kyoto) 1991;50:294–7.

[12] Harcourt JP, Brookes GB. Delayed endolymphatic hydrops: clinical manifestations and treatment outcome. Clin Otolaryngol 1995;20:318–22.

[13] Sawada S, Takeda T, Kakigi A, Saito H. Delayed endolymphatic hydrops (DEH). Pract Otol (Kyoto) 1995;88:1129–34.

[14] Takeda N, Koizuka I, Nishiike S, Kitahara T, Horii S, Uno A, et al. Clinical features in patients with delayed endolymphatic hydrops. J Otolaryngol Jpn 1998;101:1385–9.

[15] Mizuta K, Ito Y, Ushida J, Mori M, Kuze B, Hayakawa K, et al. Clinical characteristics of delayed endolymphatic hydrops. Equilibrium Res (Kyoto) 1998;57:328–34.

[16] Huang TS, Lin CC. Delayed endolymphatic hydrops: study and review of clinical implications and surgical treatment. Ear Nose Throat J 2001;80:76–91.

[17] Komatsuzaki A, Futaki T, Harada Y, Hozawa J, Ishii T, Kamei T, et al. Delayed endolymphatic hydrops. The guideline for standardization of diagnostic criteria in vertiginous diseases. The Committee for Standardization of Diagnostic Criteria in 16 Vertiginous Diseases. Equilibrium Res (Kyoto) 1987;47:249–50.

[18] Schuknecht H. 1985. Neurolabyrinthitis. Viral infections of the peripheral auditory and vestibular systems. In: Nomura Y, editor. Hearing loss and dizziness. Tokyo: Igaku-Shoin, p 1–12.

[19] Merchant SN, Durand ML, Adams JC. Sudden deafness: is it viral? ORL J Otorhinolaryngol Relat Spec 2008;70:52–60.

[20] Shojaku H, Watanabe Y, Yagi T, Takahashi M, Takeda T, Ikezono T, et al. Changes in the characteristics of definite Meniere's disease over time in Japan: a long-term survey by the Peripheral Vestibular Disorder Research Committee of Japan, formerly the Meniere's Disease Research Committee of Japan. Acta Otolaryngol 2009;129:155–60.

[21] Paparella MM, Mancini F. Trauma and Meniere's syndromes. Laryngoscope 1983;93:1004–12.

[22] Ylikoski J. Delayed endolymphatic hydrops syndromes after heavy exposure to impulse noise. Am J Otol 1988;9:282–5.

[23] Suzuki M, Hanamitsu M, Kitanishi T, Kohzak H, Kitano H. Autoantibodies against inner ear proteins in patients with delayed endolymphatic hydrops and unilateral juvenile deafness. Acta Otolaryngol 2006;12:117–21.

Eur Arch Otorhinolaryngol
DOI 10.1007/s00405-011-1484-3

OTOLOGY

Acoustic overstimulation-induced apoptosis in fibrocytes of the cochlear spiral limbus of mice

Yong Cui · Guang-wei Sun · Daisuke Yamashita · Sho Kanzaki · Tatsuo Matsunaga · Masato Fujii · Kimitaka Kaga · Kaoru Ogawa

Received: 10 July 2010 / Accepted: 6 January 2011

Abstract Fibrocytes of the spiral limbus are thought to play a significant role in maintaining ion homeostasis in the cochlea. The present study measured physiological and morphological changes in spiral limbus of mice in response to noise exposure. 6-week-old male C3H/HeJJcl mice were exposed to octave-band noise (120 dB SPL) for 2 h and evaluated at a series of times thereafter, up to 8 weeks. Permanent hearing loss resulted in the mice, as assessed by auditory brainstem response (ABR) recordings. The fibrocytes loss was found in the spiral limbus of the apical turn, which has been proved to be induced by apoptosis. These results suggest that noise exposure might result in apoptosis of fibrocytes in spiral limbus, which suggest a mechanism for noise-induced hearing loss.

Keywords Spiral limbus · Fibrocytes · Noise · Hearing loss

Yong Cui and Guang-wei Sun equally contributed to this work.

Y. Cui · D. Yamashita · S. Kanzaki · K. Ogawa
Department of Otolaryngology,
School of Medicine, Keio University,
35 Shinanomachi, Shinjuku-ku,
Tokyo 160-8582, Japan

Y. Cui · G. Sun · D. Yamashita · T. Matsunaga · M. Fujii · K. Kaga
Laboratory of Auditory Disorders,
Division of Hearing and Balance Research,
National Institute of Sensory Organs,
National Tokyo Medical Center,
2-5-1 Higashigaoka, Meguro-ku,
Tokyo 152-8902, Japan

Y. Cui
Department of Otolaryngology,
Guangdong Academy of Medical Sciences
& Guangdong General Hospital,
106 Zhongshan Second Road,
Guangzhou 510080, People's Republic of China

G. Sun (✉)
Lab of Biomedical Material Engineering,
Dalian Institute of Chemical Physics,
The Chinese Academy of Sciences,
457 Zhongshan Rd, Dalian 116023, China
e-mail: sunrise124@gmail.com

Published online: 19 January 2011

Introduction

Histopathology associated with noise-induced hearing loss has been studied extensively and most of the research generally focused on pathological alterations in the hair cells and stereocilia [1–3]. The damage to other sensory structures, for example, afferent dendrites, and spiral ganglion cells (SGCs) can also lead to hearing loss [4, 5].

The functions of hair cells depend on the ionic homeostasis (especially K^+) in the endolymph, which is maintained by the K^+ recycling in the inner ear. The lateral wall and spiral limbus in the cochlea play an important role in the K^+ recycling, which can transport the K^+ ions actively by ion-exchange enzyme systems [6].

Hirose and colleagues [1, 7] characterized noise injury extending beyond the sensory structures to non-sensory structures (strial vascularis, spiral ligament and spiral limbus). In mice and other models, the morphological, enzymatic, and cytochemical features of the lateral wall, especially the stria, changed markedly hours and days after noise exposure [8–10].

Although the pathological change in the spiral limbus has been reported previously [1, 11–13], the time course of those morphological changes and the mechanism under them have not been well studied. In the present study, we tried to answer those questions.

Materials and methods

Animals and experimental groups

Male C3H/HeJJcl mice aged 6 weeks were used in the present study. Previous study showed that C3H mouse maintained excellent cochlear function throughout the first year of his age [14]. Animals were randomly assigned to serve as control or as noise-exposed subjects. The experimental groups included the following nine groups of mice ($n = 3$ per group) that were assessed 0, 6, 12, 24 h, 3 days, 1, 2, 4 and 8 weeks, respectively, after noise exposure. All mice underwent auditory brainstem response (ABR) threshold testing before being exposed to noise and immediately prior to killing. All experiments were conducted in accordance with the guidelines of the National Institutes of Health and the Declaration of Helsinki, and guidelines set by the Keio University Union on Laboratory Animal Medicine.

Noise exposure

Mice from each experimental group were placed in a custom-made sound chamber fixed within individual compartments of a metallic mesh cage which can hold four animals. The sound chamber was fitted with a speaker driven by a noise generator (AA-67N; RION Co., Ltd., Tokyo, Japan) and two power amplifiers (SRP-P150; Sony, Tokyo, Japan, and D-1405; Fostex, Chesterfield, MO). In all the experimental groups, the animals were exposed to one octave-band noise centered at 4 kHz, at 120 dB SPL for 2 h. Sound levels were calibrated and measured with a sound level meter (NL-20; RION Co., Ltd., Tokyo, Japan) placed at the level of the animal's head.

Auditory brainstem response (ABR) recordings

Auditory brainstem responses were evoked as described previously [15]. ABR recordings were performed with an extracellular amplifier Digital Bioamp system (BAL-1; Tucker-Davis Technologies, Alachua, FL), and waveform storing and stimulus control were performed with PowerLab systems Scope software (PowerLab 2/20; ADInstruments, Castle Hill, Australia). Sound stimuli were produced with a coupler type speaker (ES1spc; Bioresearch Center, Nagoya, Japan), which was inserted into the external auditory canal of each mouse. Mice were anesthetized with ketamine (80 mg/kg, i.p.) and xylazine (15 mg/kg, i.p.), and then implanted with stainless steel needle electrodes, which were placed at the vertex and ventrolateral to the left and right ears. Tone burst stimuli (0.1 ms rise/fall time; 1 ms flat segment) were used as test tones. Generally, the ABR waveforms were recorded for 12.8 ms at a sampling rate of 40,000 Hz using 50–5,000 Hz band-pass filter settings; waveforms from 1,024 stimuli at a frequency of 9 Hz were averaged. The ABR waveforms were recorded at 5 dB SPL intervals. The stimulus threshold was defined as the lowest sound level at which a recognizable waveform could still be seen. Because the sound level of test tones generated from the machine is limited, we set the stimulus threshold to 89.7, 91.7, and 83.2 dB SPL at 4, 8, and 16 kHz, respectively, when a mouse failed to respond due to profound noise-induced hearing impairment. The left and right ears of each mouse were used for ABR recording.

Histological preparations

After anesthetization with xylazine (15 mg/kg, i.p.) and ketamine (80 mg/kg), the animals were perfused transcardially with cold 0.01 M phosphate-buffered saline (PBS; pH 7.4), followed by 4% paraformaldehyde in 0.1 M PB. The left cochleas were extracted ($n = 3$, each time point), and a hole was made in the apex to allow intra-labyrinthine perfusion with the fixative. After overnight post-fixation in the same fixative at 4°C, cochleas were decalcified with buffered 0.1 M ethylenediaminetetraacetate (EDTA, pH 7.5) for 1 week at 4°C. Cochleas were dehydrated through a graded ethanol series and xylene, embedded in paraffin, and then sectioned in the midmodiolar plane at 5.0 μm. Light microscope: the slides containing cochlea sections were stained with hematoxylin and eosin (H&E) (Sakura Finetek Japan, Tokyo, Japan) to view the structure. The specimens were viewed with a laboratory microscope (DM 2500; Leica, Houston, TX). In the present study, the cochlea was divided into four half turns (lower basal, upper basal, lower apical, and upper apical). The fibrocytes in the spiral limbus of the lower apical turn were counted.

The cell density calculation was performed as described previously [16]. The cell density of fibrocytes in the spiral limbus, lateral wall and SGCs within the lower apical turn was calculated after H&E staining ($n = 15$, each time point). Area measurement and cell count were performed using ImageJ, a java-based image analysis program developed at the US National Institutes of Health.

Apoptosis detection

The TUNEL assay was performed with an apoptosis in situ detection kit (Wako, Osaka, Japan) according to the manufacturer's instructions ($n = 3$, each group). Negative controls were subjected to proteinase K digestion but not terminal deoxynucleotidyl transferase (TdT) treatment. Distilled water was substituted for TdT reagent in the negative controls.

The detection of anti-single-stranded DNA (ssDNA) was done as follows: after deparaffinization, the sections were

blocked with 10% normal goat serum (Sigma–Aldrich, St. Louis, MO) diluted in 0.01 M PBS for 60 min at room temperature. Incubation with primary and secondary antibodies was carried out in PBS containing 1% normal goat serum overnight at 4°C or for 1 h at room temperature. For negative controls, the primary antibody was omitted. Nuclear staining was performed with 4′6-diamidino-2-phenylindole dihydrochoride (DAPI, 1:1000; Sigma–Aldrich). The working dilutions and sources of the antibodies used in this study were as follows: rabbit ssDNA (1:200; Dako, Kyoto, Japan), Alexa Fluor 488 goat anti-mouse IgG (1:500; Molecular Probes, Eugene, OR,).

All tissue sections for one experiment were incubated for exactly the same time in all steps, and all images were collected using the same settings; thus, the differences in the intensity of staining reflect differences in the amount of bound antibody.

Statistical analysis

All statistical analyses were performed using one-way analysis of variance. SPSS 14.0 (SPSS for Windows; SPSS Inc., Chicago, IL, USA) was used for comparisons between experimental groups and control groups. $P < 0.01$ was considered significant.

Results

ABR recordings

ABR thresholds were recorded from control and seven groups of mice. Before noise exposure, each animal showed normal cochlear function (Fig. 1). For the noise-exposed groups, ABRs were recorded 0 h, 24 h, 3 days, 1, 2, 4, and 8 weeks, respectively, after noise exposure. Immediately after acoustic trauma (0 h) in the noise-exposed animals, the average threshold shift was 61.67, 88.33, and 79.17 dB SPL at 4, 8, and 16 kHz. Twenty-four hours after acoustic trauma, the threshold shift partially recovered and remained at this level for 8 weeks (Fig. 1). The stable threshold shift at 8 weeks after noise exposure suggested that the hearing loss in this model represents a permanent threshold shift (PTS).

Tissue processing for histology

To investigate the mechanism underlying noise-induced hearing loss, we stained cochlea from the noise-exposed mice with H&E stain and examined the cochlea for histopathological changes.

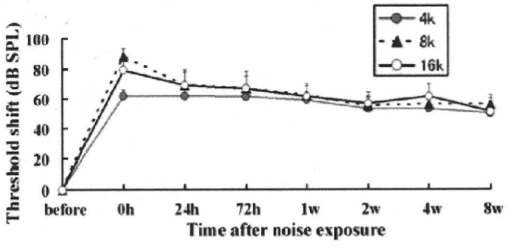

Fig. 1 Time course of threshold shifts following exposure to a one octave-band noise (centered at 4 kHz, 120 dB SPL) for 2 h. Threshold shifts were measured by recording auditory brainstem evoked responses (ABRs). ABR threshold increased immediately after noise exposure but recovered partially after 24 h and remained at this diminished level until the final ABR recording session (8 weeks after noise exposure), indicating that this type of acoustic trauma caused permanent hearing loss

Twelve hours after acoustic trauma, degenerating fibrocytes were present in spiral limbus within the apical turn of the cochlea; these cells displayed nuclear pyknosis and cytoplasmic vacuolation (Fig. 2f). Twenty-four hours after acoustic trauma, almost all fibrocytes in this region were gone (Fig. 2g). No recovery of fibrocytes was observed, even at 8 weeks (Fig. 2h).

By contrast, fibrocytes in the spiral limbus within the basal turn of the cochlea remained intact and displayed no apparent degenerative changes (Fig. 2b). Interdental cells in the spiral limbus were also unaffected by noise exposure; we did not observe degenerative changes during the entire observation period (Fig. 2).

In addition, under light microscopy, lateral wall, organ of Corti, SGCs appeared structurally well preserved at all time points following noise exposure (Fig. 2).

The number of fibrocytes in the spiral limbus and SGCs

Next, we quantified the cell number within the apical turn of the cochlea at seven time points after noise exposure, including the fibrocytes in the limbus, the SGCs, and the cells in lateral wall (Fig. 3). Since the upper apical turns in some preparations were destroyed as a result of the fixation procedure (a hole was made in the apex to facilitate fixation), we counted fibrocytes in the lower apical turn and SGCs. Five series of slides through mid-modiolus for each cochlea were used for cell counting ($n = 3$ cochleas).

For fibrocytes in the limbus, there was no significant fibrocytes loss 0 and 6 h after noise exposure. Twelve hours after exposure and thereafter, however, the number of fibrocytes in the spiral limbus decreased dramatically compared to that in the control group ($P < 0.01$) (Fig. 3a).